Progress In Electromagnetics Research, PIER 27, 337–356, 2000

EFFICIENT EVALUATION OF MODAL GREEN'S FUNCTIONS ARISING IN EM SCATTERING BY BODIES OF REVOLUTION

Alaa. K. Abdelmageed

Engineering Mathematics and Physics Department
Cairo University
Giza 12211, Egypt

1. INTRODUCTION

The problem of electromagnetic scattering by a body of revolution (BOR) has been given a great attention due to its significance in radar applications and geophysical exploration. A BOR is a three-dimensional object which is formed by rotating a planar curve called the generating arc about the axis of symmetry. By taking the advantage of the rotational symmetry of the BOR, the problem can thus be reduced from the three-dimensional case to a series of two-dimensional problems. This results in a considerable saving in both the time of computation and memory storage. This problem has been tackled by many works like [1–3] for both the conducting and dielectric objects. In these works, an integral equation is formulated with the subsequent application of the moment method.

The computation time consumed in solving the integral equation of the BOR depends primarily on the evaluation of what are called the modal Green's functions (MGF). In the above-mentioned references, these functions are evaluated using an adaptive numerical integration method. Any saving in time while computing these functions will affect the overall time of computation. Gedney and Mittra [4] used the FFT technique to enhance the computational efficiency of the moment method. However, this enhanced efficiency is obtained at the expense of the increase of the required memory storage.

Wang [5] obtained an exact expression for the kernel of cylindrical antenna. Werner [6] used a similar procedure to obtain an exact formulation for the vector potential of a cylindrical dipole antenna with a uniformly distributed current and arbitrary radius. He [7] also derived an exact integration procedure for thin circular loop antennas. Recently, Werner [8] used the same procedure to analyze a moderately thick cylindrical wire antenna.

In this paper, we extend the procedure adopted by Wang and Werner to express the MGF in terms of an exact series form. In order to enhance the convergence of the obtained series, we resort to acceleration methods which are also called transformation techniques. The essence of these techniques is to transform a slowly converging sequence of partial sums to a new faster converging one. A good review of these methods is found in [9–11]. There are many methods like Euler's transformation, Aitken's Δ^2 transformation, Shanks' transformation, θ-algorithm, $\cdots$ etc. To select the candidate method for a certain type of sequence, one has to try different methods and choose the one which gives best results. In our work, we found that the Aitken's Δ^2 transformation yields the best results. Although the new method is applicable to both the conducting and dielectric BORs, we will confine our discussion here to the conducting BORs.

The paper is organized as follows. In Section 2, the integral equations of an EM scattering by a PEC BOR in free space is presented. In Section 3, an exact series form for the modal Green's functions is derived. The convergence of this series form is studied in Section 4. Numerical results are given in Section 5. Some concluding remarks are included in Section 6.

2. THE INTEGRAL EQUATIONS OF A PEC BOR

Consider the BOR illustrated in Fig. 1, where it is formed by rotating a planar curve, called the "generating arc", around the z-axis which is also called the axis of the BOR. The t-coordinate, which is shown in Fig. 1, follows the generating arc on the body surface S. The BOR is immersed in a free space of permittivity ϵ_o, permeability μ_o, wavenumber $k_o = \omega\sqrt{\mu_o\epsilon_o}$ and intrinsic impedance $\eta_o = \sqrt{\mu_o/\epsilon_o}$. The boundary conditions state that the tangential electric field must vanish on the surface S, i.e.,

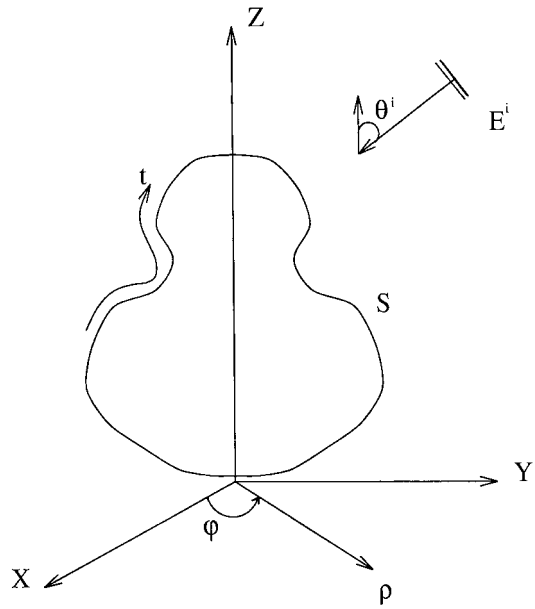

Figure 1. Geometry of a body of revolution.

$$\hat{\boldsymbol{n}} \times \left[\boldsymbol{E}^s(\boldsymbol{r}) + \boldsymbol{E}^i(\boldsymbol{r})\right] = 0 \tag{1}$$

where $\hat{\boldsymbol{n}}$ is the outward unit normal vector, $\boldsymbol{E}^S$ is the scattered field and $\boldsymbol{E}^i$ is the incident field. The scattered field can be expressed as

$$\boldsymbol{E}^s(\boldsymbol{r}) = -j\omega\boldsymbol{A}(\boldsymbol{r}) - \boldsymbol{\nabla}\Phi(\boldsymbol{r}) \tag{2}$$

where $\boldsymbol{A}(\boldsymbol{r})$ and $\Phi(\boldsymbol{r})$ represent the vector and scalar potentials,

respectively. They are defined by

$$\boldsymbol{A}(\boldsymbol{r}) = \frac{\mu_o}{4\pi} \int dS'\, G(\boldsymbol{r}\,|\,\boldsymbol{r}')\boldsymbol{K}(\boldsymbol{r}') \tag{3}$$

$$\Phi(\boldsymbol{r}) = \frac{j}{4\pi\omega\epsilon_o} \int dS'\, G(\boldsymbol{r}\,|\,\boldsymbol{r}')\boldsymbol{\nabla}' \cdot \boldsymbol{K}(\boldsymbol{r}') \tag{4}$$

where G is given by

$$G(\boldsymbol{r}\,|\,\boldsymbol{r}') = \frac{e^{-jk_oR}}{R} \tag{5}$$

and $R = |\boldsymbol{r}-\boldsymbol{r}'|$. $\boldsymbol{r}$ and $\boldsymbol{r}'$ are the position vectors of the field and source points, respectively. $\boldsymbol{K}(r')$ is the electric surface current density. The time variation $e^{j\omega t}$ is assumed and suppressed. Combining (1)–(4), we arrive at

$$\begin{aligned}\hat{\boldsymbol{n}} \times \boldsymbol{E}^i(\boldsymbol{r}) =& \frac{j\omega\mu_o}{4\pi}\Bigg[\hat{\boldsymbol{n}} \times \int dS'\, G(\boldsymbol{r}\,|\,\boldsymbol{r}')\boldsymbol{K}(\boldsymbol{r}') \\ &+ \frac{1}{k_o^2}\hat{\boldsymbol{n}} \times \boldsymbol{\nabla} \int dS'\, G(\boldsymbol{r}\,|\,\boldsymbol{r}')\boldsymbol{\nabla}' \cdot \boldsymbol{K}(\boldsymbol{r}')\Bigg]\end{aligned} \tag{6}$$

Introducing a coordinate system (t, φ), where φ is the azimuthal angle as illustrated in Fig. 1, then the integral equation (6), governing the surface current on the BOR, may be split into a set of two coupled equations as

$$\begin{aligned}\hat{\boldsymbol{t}} \cdot \boldsymbol{E}^i(\boldsymbol{r}) =& \frac{j\omega\mu_o}{4\pi}\hat{\boldsymbol{t}} \cdot \Bigg[\int dS'\, G(\boldsymbol{r}\,|\,\boldsymbol{r}')\boldsymbol{K}(\boldsymbol{r}') \\ &+ \frac{1}{k_o^2}\boldsymbol{\nabla} \int dS'\, G(\boldsymbol{r}\,|\,\boldsymbol{r}')\boldsymbol{\nabla}' \cdot \boldsymbol{K}(\boldsymbol{r}')\Bigg]\end{aligned} \tag{7}$$

$$\begin{aligned}\hat{\boldsymbol{\varphi}} \cdot \boldsymbol{E}^i(\boldsymbol{r}) =& \frac{j\omega\mu_o}{4\pi}\hat{\boldsymbol{\varphi}} \cdot \Bigg[\int dS'\, G(\boldsymbol{r}\,|\,\boldsymbol{r}')\boldsymbol{K}(\boldsymbol{r}') \\ &+ \frac{1}{k_o^2}\boldsymbol{\nabla} \int dS'\, G(\boldsymbol{r}\,|\,\boldsymbol{r}')\boldsymbol{\nabla}' \cdot \boldsymbol{K}(\boldsymbol{r}')\Bigg]\end{aligned} \tag{8}$$

$\hat{\boldsymbol{t}}$ and $\hat{\boldsymbol{\varphi}}$ are unit vectors in the t and φ directions, respectively. Taking advantage of the rotational symmetry in the problem, the currents, incident fields and scalar Green's functions are expanded in Fourier series in φ.

$$\boldsymbol{E}^i(\boldsymbol{r}) = \sum_{m=-\infty}^{\infty} \left[E_t^{im}(t)\hat{\boldsymbol{t}} + E_\varphi^{im}(t)\hat{\boldsymbol{\varphi}}\right] e^{jm\varphi} \tag{9}$$

$$\boldsymbol{K}(\boldsymbol{r}) = K_t\hat{t} + K_\varphi\hat{\varphi} = \sum_{m=-\infty}^{\infty} \left[K_t^m(t)\hat{\boldsymbol{t}} + K_\varphi^m(t)\hat{\boldsymbol{\varphi}}\right] e^{jm\varphi} \tag{10}$$

$$G(|\boldsymbol{r} - \boldsymbol{r}'|) = \sum_{m=-\infty}^{\infty} G^m(t,t')e^{jm(\varphi-\varphi')} \tag{11}$$

where the modal Green's function $G^m(t,t')$ is defined as

$$G^m(t,t') = \frac{1}{2\pi}\int_{-\pi}^{\pi} d(\varphi-\varphi')\frac{e^{-jk_oR}}{R}e^{-jm(\varphi-\varphi')} \tag{12}$$

K_t and K_φ are the current density components in the t and φ directions, respectively. K_t^m (E_t^{im}) and K_φ^m (E_φ^{im}) represent the modal current density (incident field) components in the t and φ directions, respectively. Substituting these expansions in (7) and (8), we get [3]

$$\begin{aligned} E_t^{im} =& \frac{jk_o\eta_o}{4}\int dt'\rho' K_t^m(t')\left[\sin\gamma\sin\gamma'\left(G^{m+1}+G^{m-1}\right)+2\cos\gamma\cos\gamma' G^m\right] \\ &- \frac{k_o\eta_o}{4}\int dt'\rho' K_\varphi^m(t')\sin\gamma\left(G^{m+1}-G^{m-1}\right) \\ &+ \frac{j\eta_o}{2k_o}\frac{\partial}{\partial t}\int dt'\left(\frac{\partial\rho' K_t^m(t')}{\partial t'} + jmK_\varphi^m(t')\right)G^m \end{aligned} \tag{13}$$

$$\begin{aligned} E_\varphi^{im} =& \frac{k_o\eta_o}{4}\int dt'\rho' K_t^m(t')\sin\gamma'\left(G^{m+1}-G^{m-1}\right) \\ &+ \frac{jk_o\eta_o}{4}\int dt'\rho' K_\varphi^m(t')\left(G^{m+1}+G^{m-1}\right) \\ &- \frac{\eta_o m}{2k_o\rho}\int dt'\left(\frac{\partial\rho' K_t^m(t')}{\partial t'} + jmK_\varphi^m(t')\right)G^m \end{aligned} \tag{14}$$

where γ is the angle between the tangent to the generating curve, $\hat{\boldsymbol{t}}$ and the z-axis, defined to be positive if $\hat{\boldsymbol{t}}$ points away from the z-axis. These two equations constitute the integral equations which govern the current distribution on the surface of a conducting BOR in free space. The solution of these two coupled equations yields the modal currents K_t^m and K_φ^m of mode m. In order to obtain the total currents K_t and K_φ, as expressed by (10), we have to solve these equations on a mode-by-mode basis, with subsequent application of the superposition principle. Although the expansion of current is an infinite series, it practically converges to the proper answer after a finite number of

modes. The number of modes depends on the angle of incidence of the plane wave and the radial dimension of the BOR [1].

3. EXACT EXPRESSION FOR THE MODAL GREEN'S FUNCTIONS

The modal Green's function (MGF), given by (12), can be reduced to

$$G^m(t,t') = \frac{1}{\pi}\int_0^{\pi} d(\varphi-\varphi')\frac{e^{-jk_oR}}{R}\cos m(\varphi-\varphi') = \frac{1}{\pi}\int_0^{\pi} d\beta\frac{e^{-jk_oR}}{R}\cos(m\beta) \tag{15}$$

where

$$R = |\boldsymbol{r}-\boldsymbol{r}'| = \sqrt{R_o^2 - 2\rho\rho'\cos\beta}, \quad \beta = \varphi-\varphi' \tag{16}$$

and

$$R_o = \sqrt{(z-z')^2+\rho^2+\rho'^2} \tag{17}$$

(ρ',φ',z') and (ρ,φ,z) are the coordinates of the source and field points, respectively. The MGF can be expressed as

$$G^m(t,t') = \frac{1}{-j\pi k_o z}\frac{d}{dz}\left[\int_0^{\pi} d\beta e^{-jk_oR}\cos(m\beta)\right] \tag{18}$$

Using Watson's formulas [12], Wang [5] deduced that

$$e^{-jk_oR} = e^{-jk_oR_o} + \sum_{n=1}^{\infty}\frac{(k_o^2\rho\rho')^n h_{n-1}^2(k_oR_o)}{n!(k_oR_o)^{n-1}}\cos^n\beta \tag{19}$$

where h_n^2 is the spherical Hankel function of the second kind of order n. Substituting (19) in (18) and making use of a recursion relation of spherical Hankel functions [13, p. 439], then we get

$$G^m(t,t') = \delta_{m,0}\frac{e^{-jk_oR_o}}{R_o} - jk_o\sum_{n=1}^{\infty}A_n^m h_n^2(k_oR_o)\left(\frac{k_o^2\rho\rho'}{k_oR_o}\right)^n \tag{20}$$

where

$$\delta_{m,0} = \begin{cases} 1 & \text{for m=0} \\ 0 & \text{otherwise} \end{cases} \tag{21}$$

and

$$A_n^m = \frac{1}{\pi n!}\int_0^{\pi} d\beta\cos(m\beta)\cos^n\beta \tag{22}$$

The evaluation of the coefficients A_n^m is considered in the Appendix, where sets of recurrence formulas are developed in order to compute successive values of A_n^m.

The spherical Hankel function $h_n^2(x)$ can be expanded as [13, p. 439]

$$h_n^2(x) = j^{n+1}\frac{e^{-jx}}{x}\sum_{p=0}^{n}\frac{(n+p)!}{p!(n-p)!}\frac{1}{(j2x)^p} \tag{23}$$

Substituting this expansion in (20), then we get

$$G^m(t,t') = \frac{e^{-jk_oR_o}}{R_o}\left[\delta_{m,0} + \sum_{n=1}^{\infty}\sum_{p=0}^{n} B_{n,p}^m \frac{(k_o^2\rho\rho')^n}{(k_oR_o)^{n+p}}\right] \tag{24}$$

where

$$B_{n,p}^m = A_n^m \frac{(n+p)!}{p!(n-p)!}\frac{j^{n-p}}{(2)^p} \tag{25}$$

Recurrence formulas can be developed in order to compute $B_{n,p}^m$ for successive values of p and n. These formulas are given as

$$B_{1,0}^m = jA_1^m \tag{26}$$

$$B_{n,p}^m = \frac{(n+p)(n-p+1)}{p}\frac{1}{j2}B_{n,p-1}^m \quad p = 1,2,3,\cdots,n \tag{27}$$

$$B_{n,p}^m = \frac{j(n+p)A_n^m B_{n-1,p}^m}{(n-p)A_{n-1}^m} \quad n = 2,3,4,\cdots \tag{28}$$

The coefficients $B_{n,p}^m$ are independent of the coordinates of the source and field points. This property is of great advantage since $B_{n,p}^m$ can be computed once, stored and then used for all points. This results in a considerable saving in the time of computation. The expression of (24) represents an exact series form for the modal Green's function $G^m(t,t')$. Although the series involves infinitely many terms, it can be practically truncated according to a specified error criteria. More about the convergence of this series form will be elucidated in the next section.

4. THE CONVERGENCE OF THE SERIES FORM

The convergence of the series form of a modal Green's function $G^m(t,t')$ depends on two arguments; namely R_o and $\rho\rho'$, as given by (24). As

noted in (16), there is a minimum value for R_o. It is given by the relation

$$R_o^2 \geq 2\rho\rho' \tag{29}$$

There is a singularity point at this minimum value, i.e., at $R_o^2 = 2\rho\rho'$. The integrand of (15) suffers a singularity problem at $R_o^2 = 2\rho\rho'$. Hence, it is expected that the series form in (24) will not converge at this value. Also, the convergence of (24) may be cumbersome near the singularity point. To obviate this problem, we follow a similar approach to that suggested by Glisson and Wilton [3] for the integrand of (15). They proposed that the singularity may be extracted as

$$G^m(t,t') = G_o^m(t,t') + \frac{1}{\pi}\int_0^\pi d\beta \frac{1}{R} \tag{30}$$

where

$$G_o^m(t,t') = \frac{1}{\pi}\int_0^\pi d\beta \left[\frac{e^{-jkR}}{R}\cos(m\beta) - \frac{1}{R}\right] \tag{31}$$

The first integral is now smooth while the second one is evaluated in closed form as the complete elliptic integral of the first kind. It is expressed as

$$\frac{1}{\pi}\int_0^\pi d\beta \frac{1}{R} = \frac{1}{\pi}\frac{1}{\sqrt{\rho\rho'}}\mathcal{R}K(\mathcal{R}^2) \tag{32}$$

where $K(\mathcal{R}^2)$ is the complete elliptic integral of the first kind [13, p. 590] and $\mathcal{R}$ is given by

$$\mathcal{R} = \frac{2\sqrt{\rho\rho'}}{\sqrt{(z-z')^2 + (\rho+\rho')^2}} \tag{33}$$

To put the first integral in (30) in a series form, we have to seek a suitable expansion for the integral

$$I_1 = \frac{1}{\pi}\int_0^\pi d\beta \frac{1}{R} \tag{34}$$

This integral may be visualized as the limit of another integral $I_2(\alpha)$ as $\alpha \to 0$. $I_2(\alpha)$ is given by

$$I_2(\alpha) = \frac{1}{\pi}\int_0^\pi d\beta \frac{e^{-j\alpha k_o R}}{R} \tag{35}$$

This integral can be put in a series form as in (24). Hence,

$$I_2(\alpha) = \frac{e^{-j\alpha k_o R_o}}{R_o}\left[1 + \sum_{n=1}^{\infty}\sum_{p=0}^{n} B_{n,p}^0 \frac{(\alpha^2 k_o^2 \rho\rho')^n}{(\alpha k_o R_o)^{n+p}}\right] \tag{36}$$

When $\alpha \to 0$, then we have

$$I_2(\alpha = 0) = I_1 = \frac{1}{R_o}\left[1 + \sum_{n=1}^{\infty}\sum_{p=0}^{n} B_{n,p}^0 \frac{(k_o^2 \rho\rho')^n}{(k_o R_o)^{n+p}}\delta_{p,n}\right] \tag{37}$$

Therefore the first integral in (30) can now be put in the series form

$$\begin{aligned} G_o^m(t,t') =& \frac{1}{R_o}\left[\left(e^{-jk_o R_o}\delta_{m,0} - 1\right)\right. \\ &\left. + \sum_{n=1}^{\infty}\sum_{p=0}^{n} \frac{(k_o^2\rho\rho')^n}{(k_o R_o)^{n+p}}\left(e^{-jk_o R_o} B_{n,p}^m - \delta_{p,n} B_{n,p}^0\right)\right] \end{aligned} \tag{38}$$

Hence, the modal Green's function $G^m(t,t')$ can be expressed as

$$\begin{aligned} G^m(t,t') =& \frac{1}{R_o}\left[\left(e^{-jk_o R_o}\delta_{m,0} - 1\right)\right. \\ &\left. + \sum_{n=1}^{\infty}\sum_{p=0}^{n} \frac{(k_o^2\rho\rho')^n}{(k_o R_o)^{n+p}}\left(e^{-jk_o R_o} B_{n,p}^m - \delta_{p,n} B_{n,p}^0\right)\right] \\ &+ \frac{1}{\pi}\frac{1}{\sqrt{\rho\rho'}}\mathcal{R}K(\mathcal{R}^2) \end{aligned} \tag{39}$$

In (39), we substituted the complete elliptic function for the second integral in (30) rather than the series form of (37) since the convergence of the latter is very slow near $R_o^2 = 2\rho\rho'$. When $t \to t'$, i.e., $\rho \to \rho'$ and $z \to z'$, $\mathcal{R} = 1$. At this value, a logarithmic singularity is encountered when computing the complete elliptic function. However, this singularity is integrable when it is integrated along the generating arc [14].

As it will be more clarified in next section, when $R_o^2/2\rho\rho'$ is not in the near vicinity of the singularity point the convergence of the series is fast. Only few terms are needed to be computed. However, when

$R_o^2/2\rho\rho'$ is in the near vicinity of the singularity point the convergence is rather slow. In order to enhance the convergence of the series in that range we use the Aitken's Δ^2 transformation [11]. In this technique if S_n, S_{n+1} and S_{n+2} are successive partial sums of the series, then an improved estimate S'_n is given by

$$S'_n = S_n - \frac{[\Delta S_n]^2}{\Delta^2 S_n} \tag{40}$$

where

$$\Delta S_n = S_{n+1} - S_n, \quad \Delta^2 S_n = S_{n+2} - 2S_{n+1} + S_n$$

This procedure can be repeated, if necessary, for a sequence of partial sums.

5. NUMERICAL RESULTS

To test the new presented series form for the modal Green's function, results of $G_o^m(t,t')$ versus the ratio $R_o^2/\rho\rho'$ are shown in Figs. 2 and 3. Results of $G_o^m(t,t')$ using Romberg method [15] as an adaptive numerical integration technique are also incorporated. In Fig. 2, results are given for $k_o^2\rho\rho' = 2.0$ and modes $m = 0, 1, 2$; while in Fig. 3, $k_o^2\rho\rho' = 20.0$ and $m = 3, 4, 5$. Viewing the results, it is evident that both the numerical integration and series form have a complete agreement. A point which deserves attention here is the CPU time for both schemes. In Figs. 4–7, T_s/T_i ratio is shown versus $R_o^2/\rho\rho'$ at a certain m. T_s is the CPU time using series form and T_i is the CPU time using numerical integration. In Figs. 4 and 5 $k_o^2\rho\rho' = 2.0$ while in Figs. 6 and 7 $k_o^2\rho\rho' = 20.0$. Results of these figures show that a great saving in time is generally obtained when using the series form scheme. In Figs. 4 and 5 and for $R_o^2/\rho\rho' < 2.5$, T_s/T_i is in the range $0.5 : 1.0$ and decreases as the ratio $R_o^2/\rho\rho'$ increases. For $R_o^2/\rho\rho' > 2.5$, T_s/T_i decreases below ~ 0.4. In Figs. 6 and 7 and for $R_o^2/\rho\rho'$ close to 2.0, T_s/T_i exceeds 1.0. However for $R_o^2/\rho\rho' > 2.4$, T_s/T_i decreases below ~ 0.3.

We have tried the series form for other extensive results, not shown here for brevity. All these results show that T_s/T_i decreases to $0.3 \sim 0.4$ for $R_o^2/\rho\rho' > 2.5$. Very close to $R_o^2/\rho\rho' = 2.0$, $T_s/T_i \simeq 1.0$ for small values of $k_o^2\rho\rho'(< 10)$ and exceeds 1.0 for higher values of $k_o^2\rho\rho'$.

The integral equations are solved using Glisson and Wilton approach for a BOR in free space [3]. The details will not be repeated here,

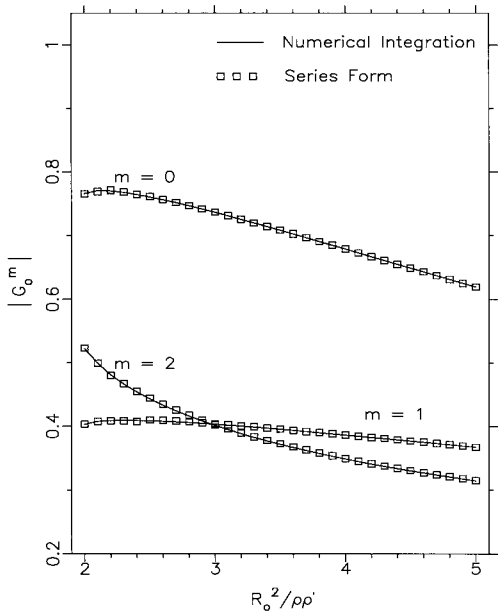

Figure 2. The computation of G_o^m for $k_o^2\rho\rho' = 2.0$.

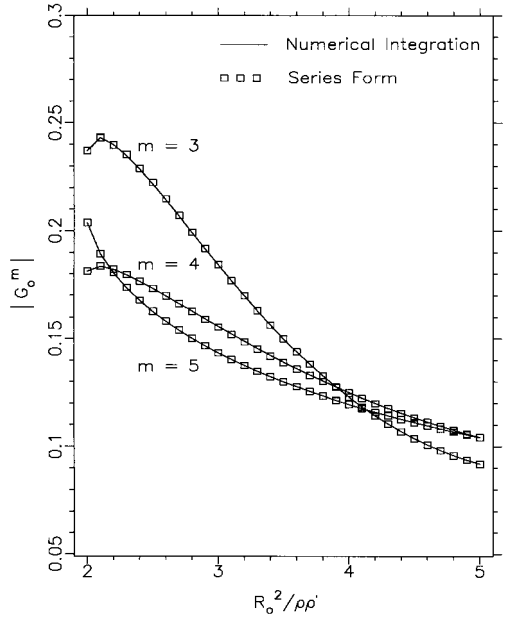

Figure 3. The computation of G_o^m for $k_o^2\rho\rho' = 20.0$.

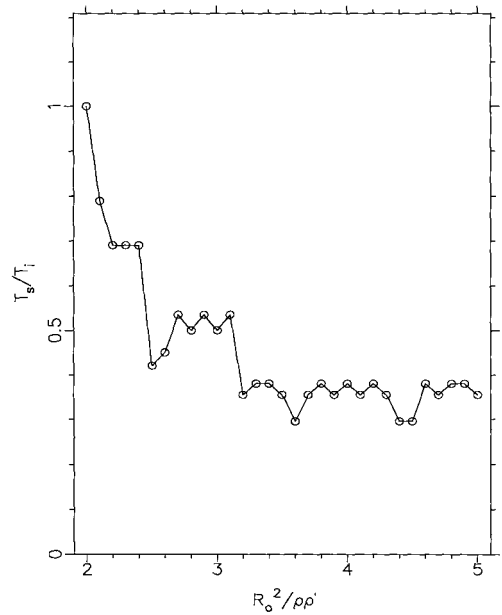

Figure 4. The CPU time ratio T_s/T_i for $k_o^2\rho\rho' = 2.0$ and $m = 0$.

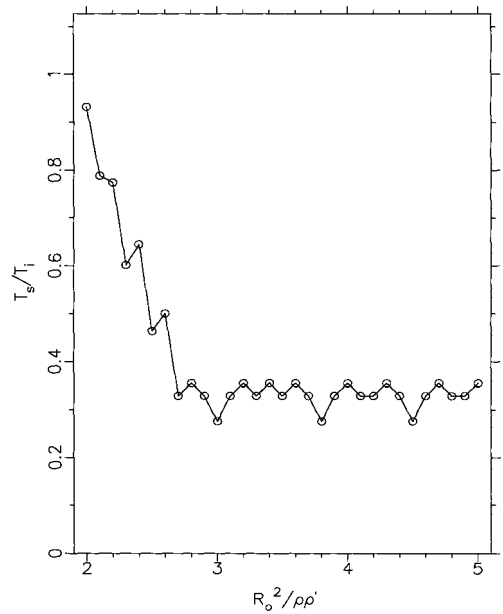

Figure 5. The CPU time ratio T_s/T_i for $k_o^2\rho\rho' = 2.0$ and $m = 2$.

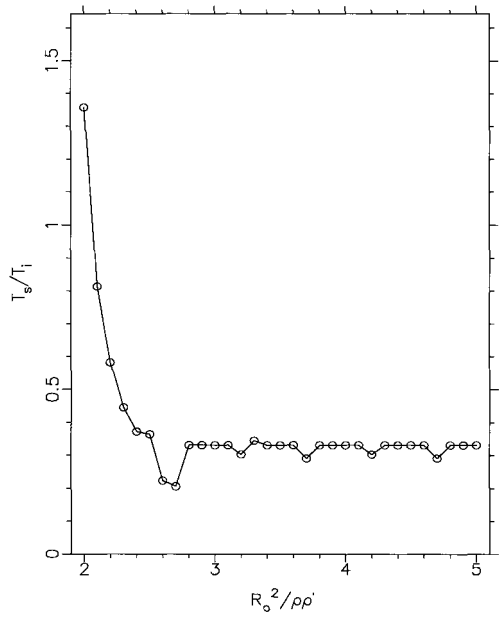

Figure 6. The CPU time ratio T_s/T_i for $k_o^2\rho\rho' = 20.0$ and $m = 4$.

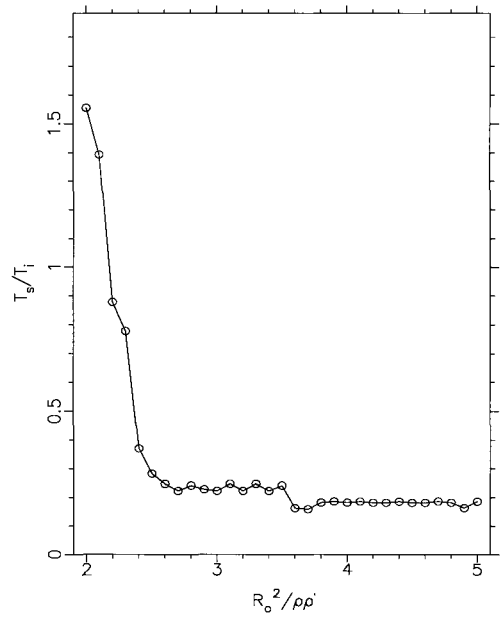

Figure 7. The CPU time ratio T_s/T_i for $k_o^2\rho\rho' = 20.0$ and $m = 5$.

and may be found elsewhere. The MGF are evaluated using both the numerical integration and series form techniques. Results of a PEC sphere of radius $a = 1.0\lambda_o$ and a PEC cylinder of radius $a = 1.0\lambda_o$, and height $h = 2.0\lambda_o$ are given in Figs. 8–11. For both cases, the BOR is illuminated with an incident plane wave at $\theta^i = 45°$. The currents are plotted versus the normalized parameter s, which runs from $s = 0(t_o)$ to $s = 1(t_f)$, where (t_o) and (t_f) are the starting and ending tips of the generating arc t. It is evident that the results using both the numerical integration and series form techniques have a good agreement.

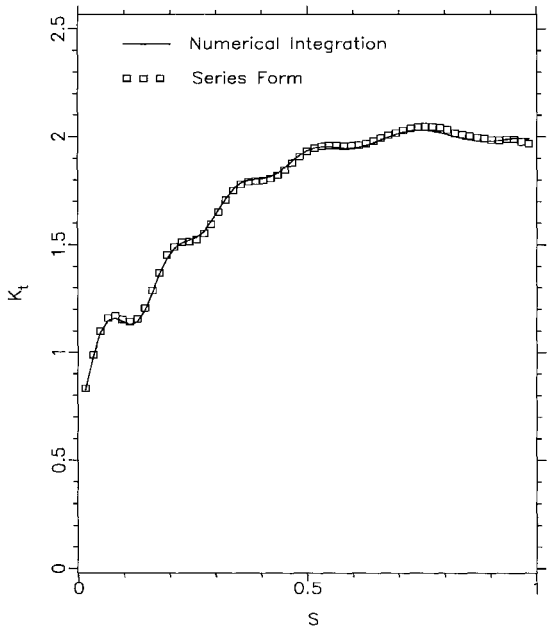

Figure 8. Magnitude of K_t on a PEC sphere of $a = 1.0\lambda_o$ illuminated by an incident plane wave at $\theta^i = 45°$ in free space.

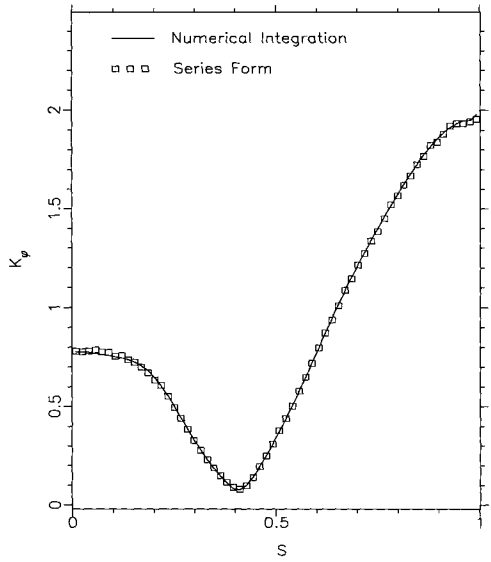

Figure 9. Magnitude of K_φ on a PEC sphere of $a = 1.0\lambda_o$ illuminated by an incident plane wave at $\theta^i = 45^\circ$ in free space.

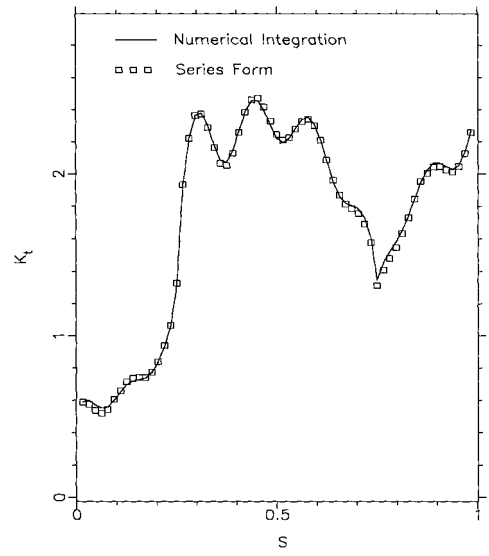

Figure 10. Magnitude of K_t on a PEC cylinder of $a = 1.0\lambda_o$ and $h = 2.0\lambda_o$ illuminated by an incident plane wave at $\theta^i = 45^\circ$ in free space.

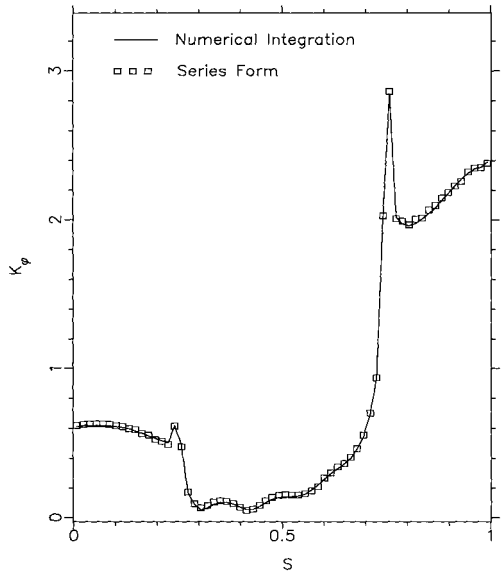

Figure 11. Magnitude of K_φ on a PEC cylinder of $a = 1.0\lambda_o$ and $h = 2.0\lambda_o$ illuminated by an incident plane wave at $\theta^i = 45^\circ$ in free space.

In Table 1, the matrix fill CPU times of PEC spheres of radii $a = 0.2\lambda_o,\ 0.5\lambda_o,\ 1.0\lambda_o$ are given for both the numerical integration and series form techniques. Table 2 also includes the matrix fill CPU times of PEC cylinders of various dimensions. For these results, $\theta^i = 45^\circ$. The number of computed modes M and the matrix size $(2N+1)$ are also given, where N is the number of segments of the generating arc. The computations using the two techniques have been implemented on a 300-MHz Pentium. Examining the CPU times, it is observed that a significant saving in time is achieved using series form.

Table 1. The matrix fill CPU time of PEC spheres in free space using both the numerical integration and series form techniques.

a λ_o	Number of Modes M	Matrix Size $2N+1$	CPU Time (sec.)	
			N. Integration	Series Form
0.2	3	43	7	3
0.5	5	63	31	15
1.0	7	123	278	103

Table 2. The matrix fill CPU time of PEC cylinders in free space using both the numerical integration and series form techniques.

a λ_o	h λ_o	Number of Modes M	Matrix Size $2N+1$	CPU Time (sec.)	
				N. Integration	Series Form
0.2	1.0	3	47	9	4
0.5	1.0	5	63	33	13
1.0	2.0	7	127	286	113

6. CONCLUSION

A new method is presented for evaluating the modal Green's functions. These functions are usually encountered when solving the problems of EM scattering by bodies of revolution. Instead of the numerical integration technique which is usually used to evaluate such functions, an exact series form is derived. To accelerate the convergence of such series we used the Aitken's Δ^2 transformation. We used this series form to study the scattering by PEC spheres and cylinders. It is shown that a great saving in the time of computation is achieved.

APPENDIX. EVALUATION OF THE COEFFICIENTS A_n^m

The coefficients A_n^m expressed by (22) involve integrals which have closed form solution [16, p. 143]. A_n^m have nonzero values when $(m+n)$ is an even integer. This means that both m and n are either even or odd integers. When m and n are both odd numbers, A_n^m are

expressed as

$$A_n^m = \left[C_n^{mo} + \sum_{q=1}^{q^o} D_{n,q}^o E_q^{mo} \right] \delta_{n,\text{odd}} \tag{41}$$

where

$$C_n^{mo} = (-1)^{(m-1)/2} m \frac{n!!}{2^{n_1} n! n_1!} \tag{42}$$

$$D_{n,q}^o = \frac{(2q+n)!!}{2^{q+n_1} n!(q+n_1)!(2q+1)!} \tag{43}$$

$$E_q^{mo} = (-1)^{q+(m-1)/2} m[m^2 - 1^2][m^2 - 3^2] \cdots [m^2 - (2q-1)^2] \tag{44}$$

and

$$n_1 = \frac{n+1}{2}, \quad q^o = \frac{m-1}{2} \tag{45}$$

$$\delta_{n,\text{odd}} = \begin{cases} 1 & \text{for } n = 1, 3, 5, \cdots \\ 0 & \text{otherwise} \end{cases} \tag{46}$$

The function $x!!$ is defined as

$$x!! = \begin{cases} 1.3.5 \cdots x & \text{for odd values of } x \\ 2.4.6 \cdots x & \text{for odd values of } x \end{cases} \tag{47}$$

For even values of both m and n, we have

$$A_n^m = \left[C_n^{me} + \sum_{q=1}^{q^e} D_{n,q}^e E_q^{me} \right] \delta_{n,\text{even}} \tag{48}$$

where

$$C_n^{me} = (-1)^{m/2} \frac{(n-1)!!}{2^{n_2} n! n_2!} \tag{49}$$

$$D_{n,q}^e = \frac{(2q+n-1)!!}{2^{q+n_2} n!(q+n_2)!(2q)!} \tag{50}$$

$$E_q^{me} = (-1)^{m/2} (-1)^q m^2 [m^2 - 2^2] \cdots [m^2 - (2q-2)^2] \tag{51}$$

where

$$n_2 = \frac{n}{2}, \quad q^e = \frac{m}{2} \tag{52}$$

$$\delta_{n,\text{even}} = \begin{cases} 1 & \text{for } n = 2, 4, 6, \cdots \\ 0 & \text{otherwise} \end{cases} \tag{53}$$

In order to enhance the computation of A_n^m, sets of recursion formulas are developed. They are given by

$$C_1^{mo} = \frac{1}{2}(-1)^{(m-1)/2} m \tag{54}$$

$$C_n^{mo} = \frac{1}{2n_1(n-1)} C_{n-2}^{mo}, \quad n = 3, 5, 7, \cdots \tag{55}$$

$$D_{1,1}^{o} = \frac{1}{16} \tag{56}$$

$$D_{n,q}^{o} = \frac{(2q+n)}{4q(q+n_1)(2q+1)} D_{n,q-1}^{o}, \quad q = 2, 3, 4, \cdots \tag{57}$$

$$D_{n,q}^{o} = \frac{(2q+n)}{2n(n-1)(q+n_1)} D_{n-2,q}^{o}, \quad n = 3, 5, 7, \cdots \tag{58}$$

$$E_1^{mo} = -(-1)^{(m-1)/2} m[m^2 - 1^2] \tag{59}$$

$$E_q^{mo} = -[m^2 - (2q-1)^2] E_{q-1}^{mo}, \quad q = 2, 3, 4, \cdots \tag{60}$$

$$C_2^{me} = \frac{1}{4}(-1)^{m/2} \tag{61}$$

$$C_n^{me} = \frac{1}{n^2} C_{n-2}^{me}, \quad n = 4, 6, 8, \cdots \tag{62}$$

$$D_{2,1}^{e} = \frac{3}{32} \tag{63}$$

$$D_{n,q}^{e} = \frac{(2q+n-1)}{4q(q+n_2)(2q-1)} D_{n,q-1}^{e}, \quad q = 2, 3, 4, \cdots \tag{64}$$

$$D_{n,q}^{e} = \frac{(2q+n-1)}{2n(n-1)(q+n_2)} D_{n-2,q}^{e}, \quad n = 4, 6, 8, \cdots \tag{65}$$

$$E_1^{me} = -(-1)^{m/2} m^2 \tag{66}$$

$$E_q^{me} = -[m^2 - (2q-1)^2] E_{q-1}^{me}, \quad q = 2, 3, 4, \cdots \tag{67}$$

ACKNOWLEDGMENT

The author would like to thank Prof. A. Mohsen for his useful comments and suggestions while preparing this work. The author acknowledges with sincere appreciation the support provided by the Alexander von Humboldt-Stiftung via the computation equipment grant.

REFERENCES

1. Andreasen, M. G., "Scattering from bodies of revolution," *IEEE Trans. Antennas Propagat.,* Vol. 13, 303–310, 1965.
2. Mautz, J. R. and R. F. Harrington, "H-field, E-field and combined field solutions for conducting bodies of revolution," *Arch. Elek. Übertragung.,* Vol. 32, 157–164, 1978.
3. Glisson, A. W. and D. R. Wilton, "Simple and efficient numerical methods for problems of electromagnetic radiation and scattering from surfaces," *IEEE Trans. Antennas Propagat.,* Vol. 28, 593–603, 1980.
4. Gedney, S. D. and R. Mittra, "The use of the FFT for the efficient solution of the problem of electromagnetic scattering by a body of revolution," *IEEE Trans. Antennas Propagat.,* Vol. 38, 313–322, 1990.
5. Wang, W., "The exact kernel for cylindrical antenna," *IEEE Trans. Antennas Propagat.,* Vol. 39, 434–435, 1991.
6. Werner, D. H., "An exact formulation for the vector potential of a cylindrical antenna with uniformly distributed current and arbitrary radius," *IEEE Trans. Antennas Propagat.,* Vol. 41, 1009–1018, 1993.
7. Werner, D. H., "An exact integration procedure for vector potentials of thin circular loop antennas," *IEEE Trans. Antennas Propagat.,* Vol. 44, 157–165, 1996.
8. Werner, D. H., "A method of moments approach for the efficient and accurate modeling of moderately thick cylindrical wire antennas," *IEEE Trans. Antennas Propagat.,* Vol. 46, 373–382, 1998.
9. Brezinski, C., "Convergence acceleration methods: the past decade," *J. Comp. Appl. Math.,* Vol. 12–13, 19–36, 1985.
10. Kinayman, N. and M. I. Aksun, "Comparative study of acceleration techniques for integrals and series in electromagnetic problems," *Radio Sci.,* Vol. 30, 1713–1722, 1995.
11. Michalski, K. A., "Extrapolation methods for Sommerfeld integral tails," *IEEE Trans. Antennas Propagat.,* Vol. 46, 1405–1418, 1998.
12. Watson, G. N., *A Treatise on the Theory of Bessel Functions,* Cambridge Univ. Press, Cambridge, U.K., 1962.
13. Abramowitz, M. and I. A. Stegun, eds., *Handbook of Mathematical Functions,* Dover, New York, 1965.
14. Glisson, A. W., *On the Development of Numerical Techniques for Treating Arbitrarily-Shaped Surfaces,* Ph.D. thesis, Univ. Mississipi, 1978.

15. Davis, P. J. and P. Rabinowitz, *Methods of Numerical Integration,* Academic Press, New York, 1984.
16. Gradshtegn, I. S. and I. M. Ryzhik, *Table of Integrals, Series, and Products,* Academic Press, New York, 1980.